Supplementary Information (SI) for Journal of Materials Chemistry A.
This journal is © The Royal Society of Chemistry 2025

Supporting Information

For

Controllable Ion-Release Separator: In-Situ Engineering of Zincophilic/Hydrophobic Interface and Solvation Regulation for Durable Zn Metal Anode

Yu Zong,‡[a,b] Haichao Chen,‡[d] Danyang Yu,[c] Lu Wang,[a] Yamei Liu,[a] Xiaofan Tian,[a] Lei Wang,[b] Kuikui Wang,[c] Xin Ning,[a] and Xiaochuan Ren*[a]*

[a]Industrial Research Institute of Nonwovens & Technical Textiles, College of Textiles & Clothing, Shandong Center for Engineered Nonwovens, Qingdao University, Qingdao 266071, China

[b]State Key Laboratory of Advanced Papermaking and Paper-based Materials, School of Light Industry Science and Engineering, South China University of Technology, Guangzhou 510640, China

[c]Qingdao Central Hospital, University of Health and Rehabilitation Sciences, Qingdao 266071, China

[d]Institute of Materials for Energy and Environment, School of Materials Science and Engineering, Qingdao University, Qingdao 266071, China

*Corresponding authors: rxchuan@qdu.edu.cn and felwang@scut.edu.cn

Contents

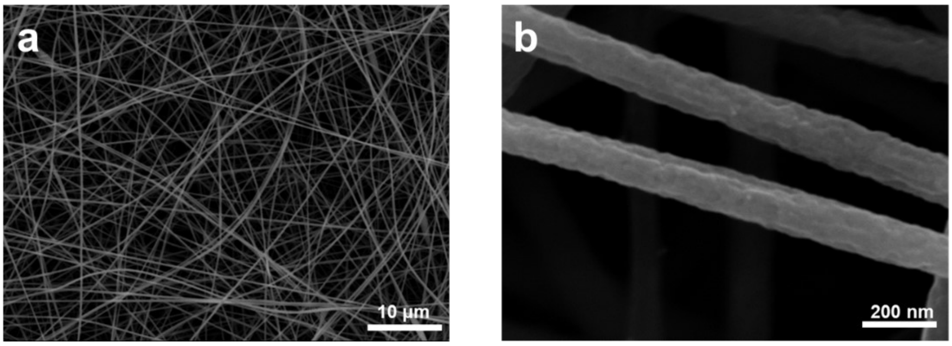

Fig. S1. a-b) SEM images of CPAN separator.

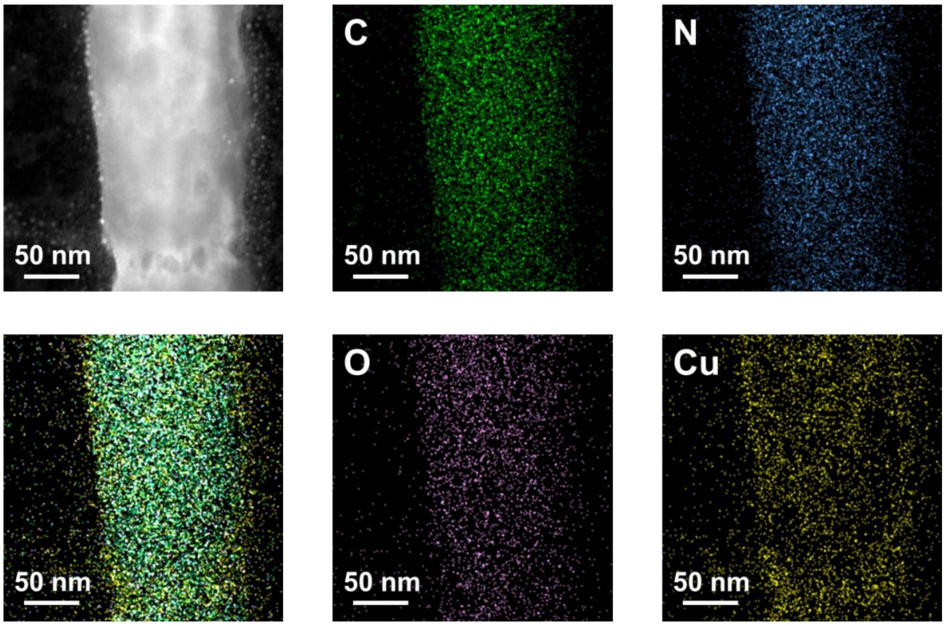

Fig. S2. The HAADF-STEM image of CPAN separator.

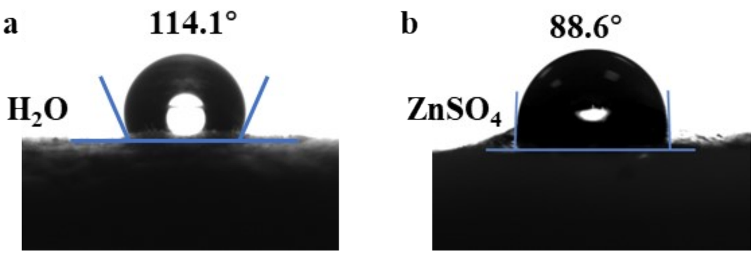

Fig. S3. The contact angle tests of (a) H_2O and (b) 2 M $ZnSO_4$ electrolyte on the PAN@Zn.

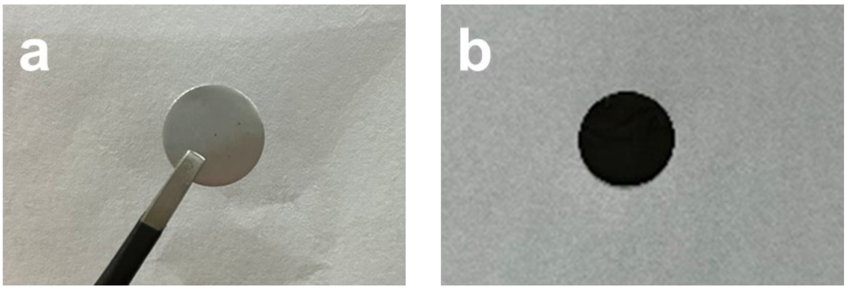

Fig. S4. Optical images of a) Zn foil and b) CuZn anode.

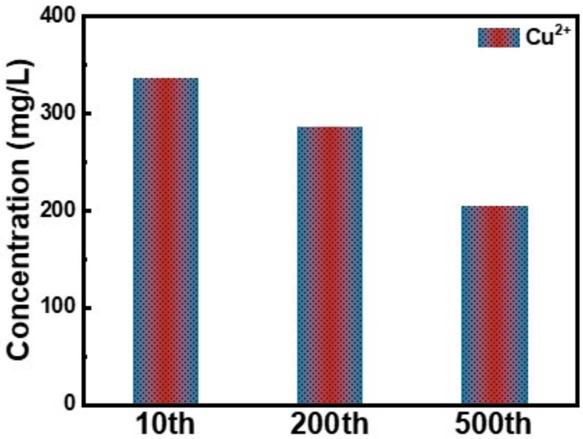

Fig. S5. Copper ion concentration in the electrolyte measured by ICP-OES at different cycles.

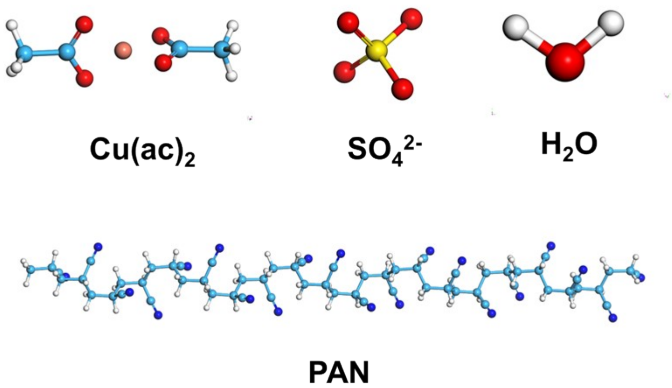

Fig. S6. The snapshots of the MD simulation for a) $Cu(Ac)_2$, b) PAN, c) SO_4^{2-} and d) H_2O.

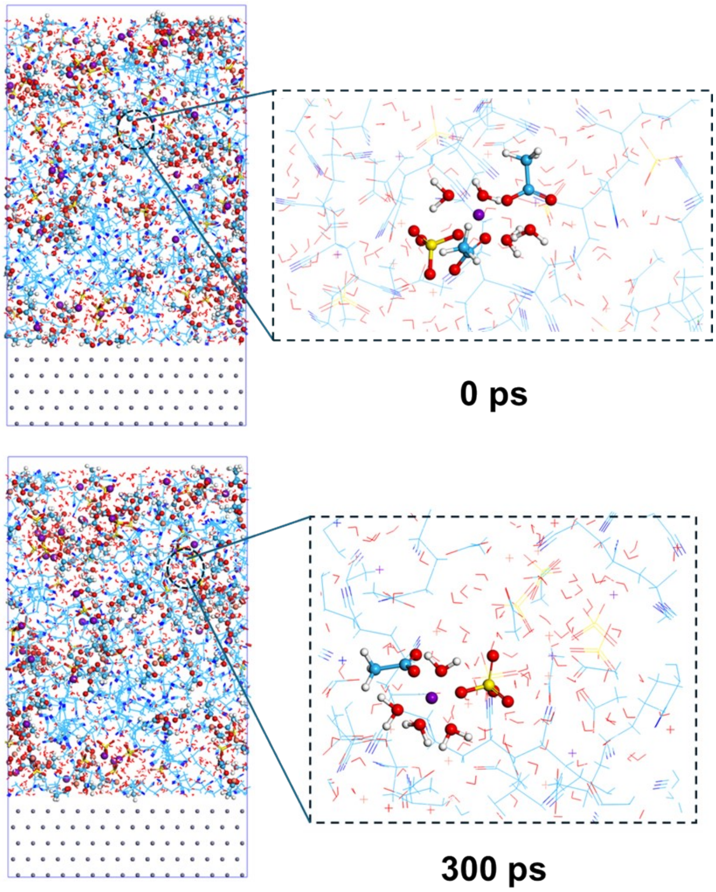

Fig. S7. The snapshots of the MD simulation of CPAN separator in $ZnSO_4$ electrolyte for 0 ps and 300 ps.

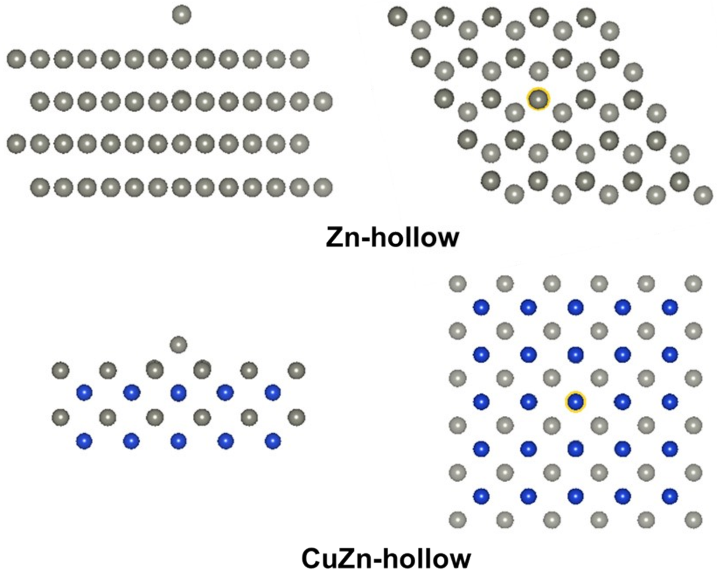

Fig. S8. The adsorption sites of zinc atom on the surfaces of Zn and CuZn alloy, respectively.

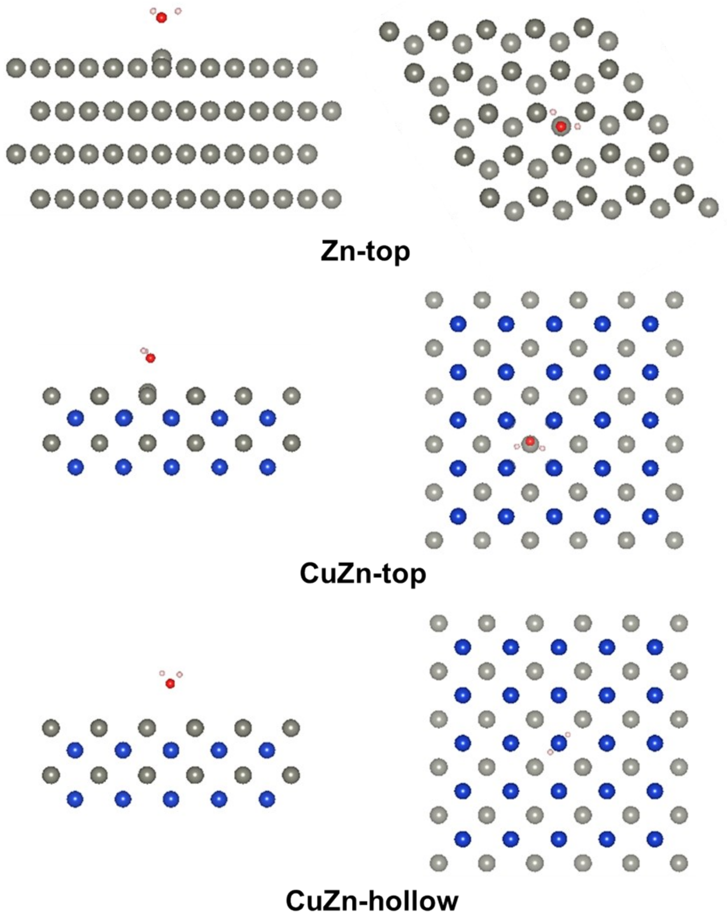

Fig. S9. The adsorption sites of H_2O on the surfaces of Zn and CuZn alloy, respectively.

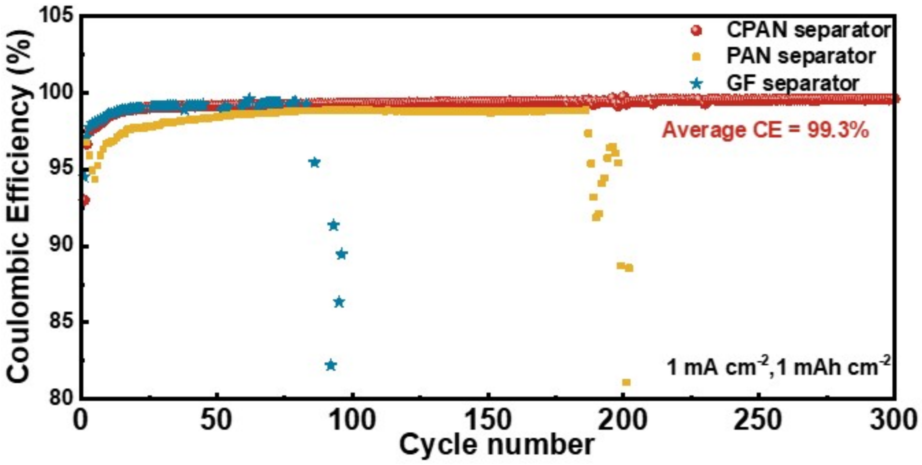

Fig. S10. Coulombic efficiencies of Zn||Cu cells with PAN separator.

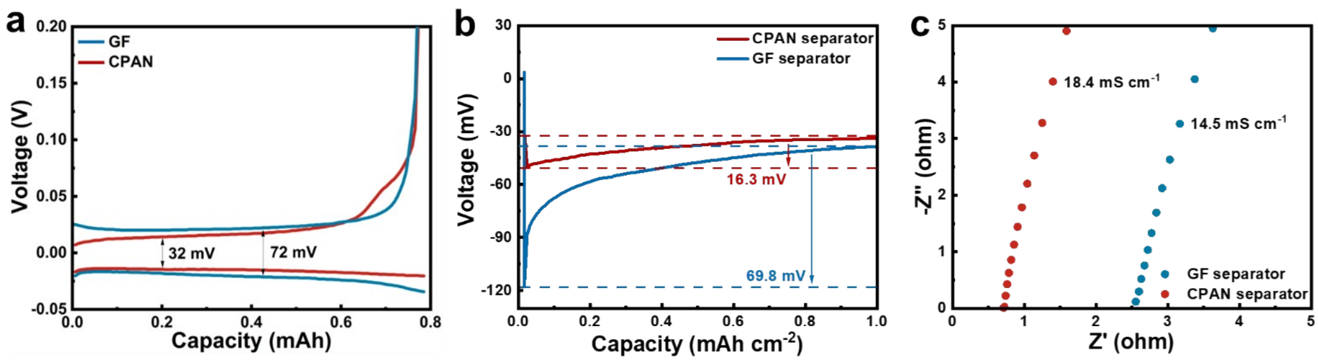

Fig. S11. (a) Voltage profiles of Zn stripping/plating process in Zn||Cu cells with different separators at 1 mA cm^{-2}, 1 mAh cm^{-2}. (b) The first cycle over potentials of Zn deposition on the bare Cu by using CPAN and GF separator, respectively. (c) Nyquist plots of GPAN, PAN, and GF with two stainless blocking electrodes and the calculated ionic conductivity.

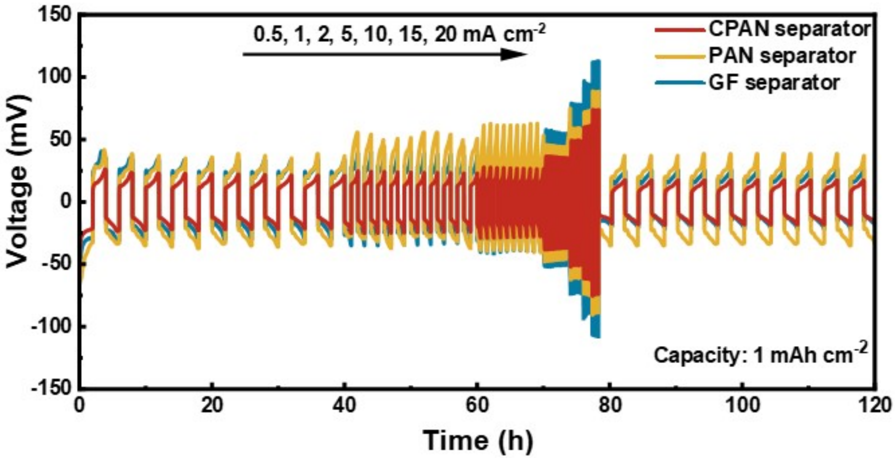

Fig. S12. Rate capability of Zn||Zn cells using different separator.

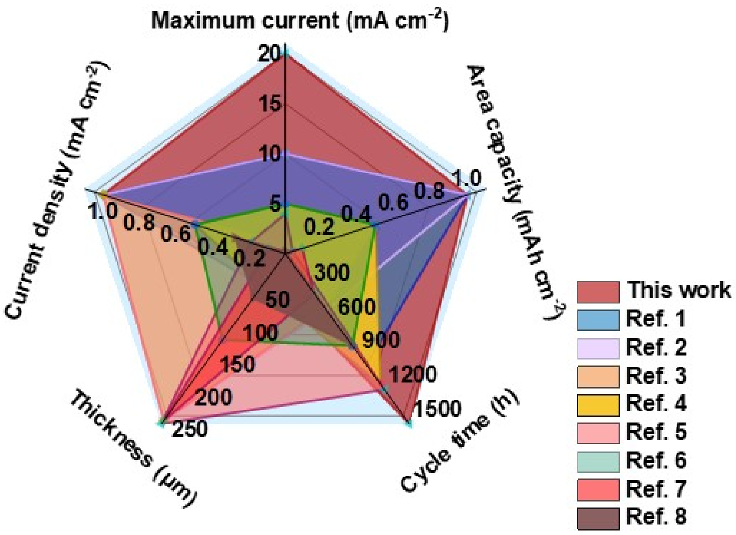

Fig. S13. Electrochemical performance of the zinc anodes coupled with different separators.[1-8] The corresponding performance values are shown in Table S1.

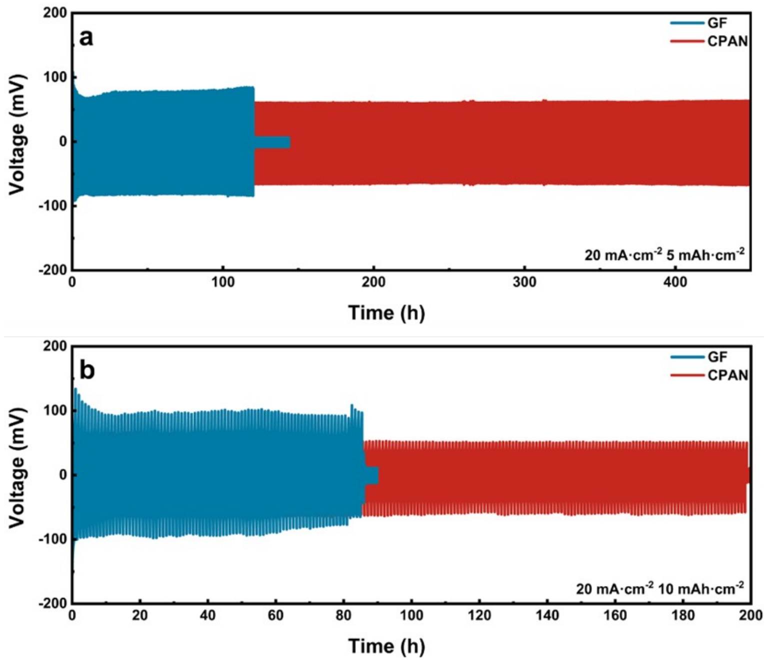

Fig. S14. Cycling performance of Zn||Zn cells with GF separator and CPAN separator at (a) 20 mA cm^{-2} with 5 mAh cm^{-2} and (b) 20 mA cm^{-2} with 10 mAh cm^{-2}.

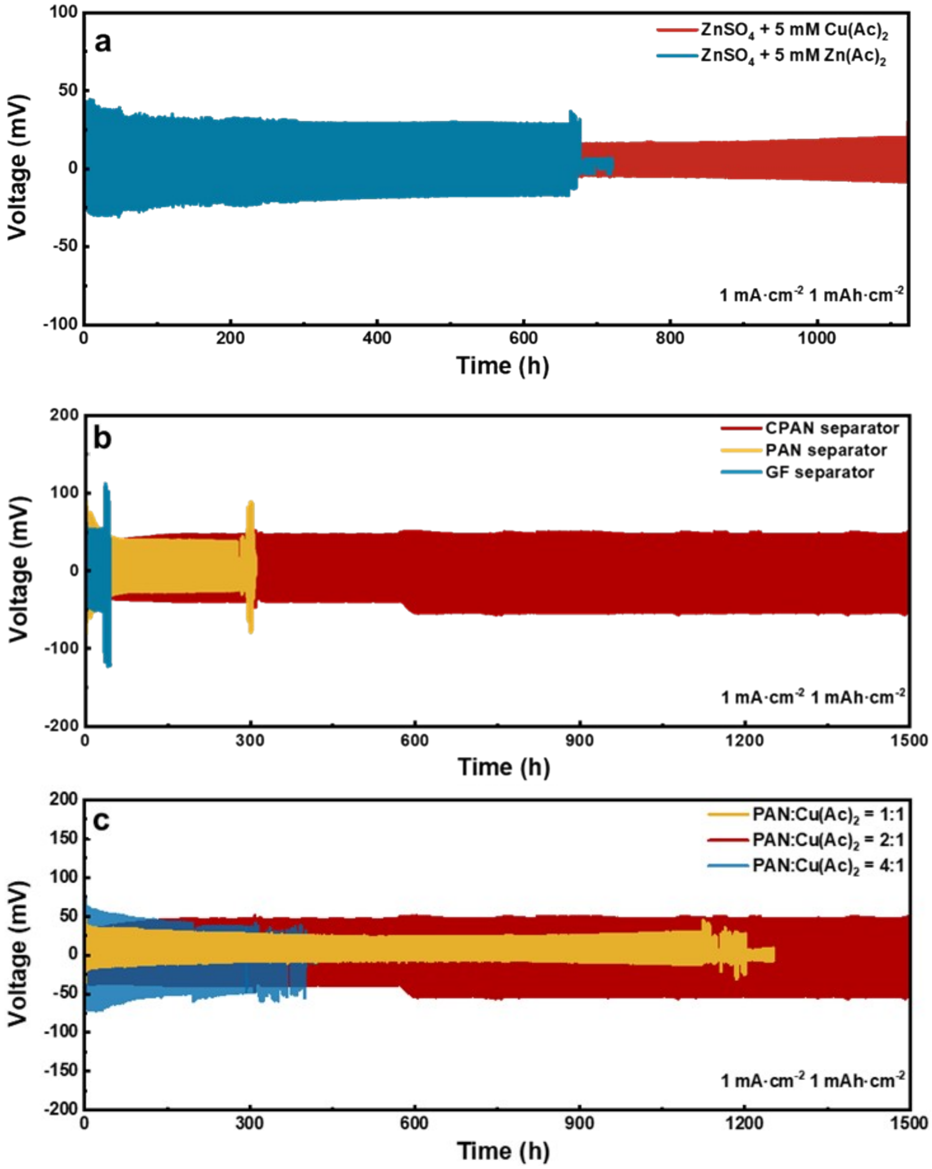

Fig. S15. (a) Long cycling performance of Zn||Zn cells using 2M $ZnSO_4$ with 5 mM $Zn(Ac)_2$ and 2M $ZnSO_4$ with 5 mM $Cu(Ac)_2$. (b) Long cycling performance of Zn||Zn cells using GF, PAN and CPAN separators. (c) Long cycling performance of Zn||Zn cells using different mass ratio of PAN: $Cu(CH_3COO)_2$.

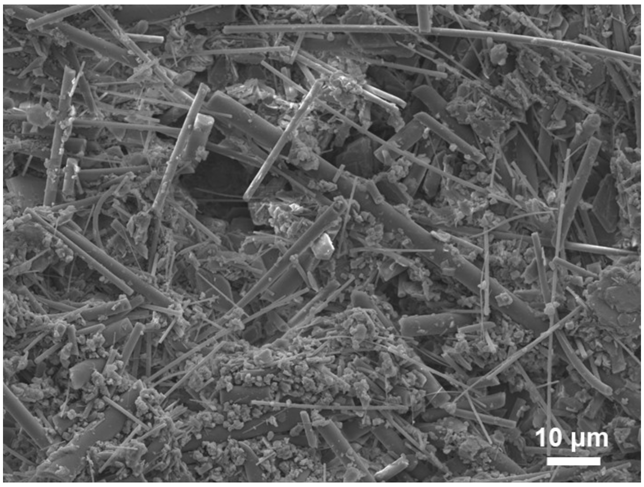

Fig. S16. Typical SEM image of Zn anode after 50 cycles with GF separator.

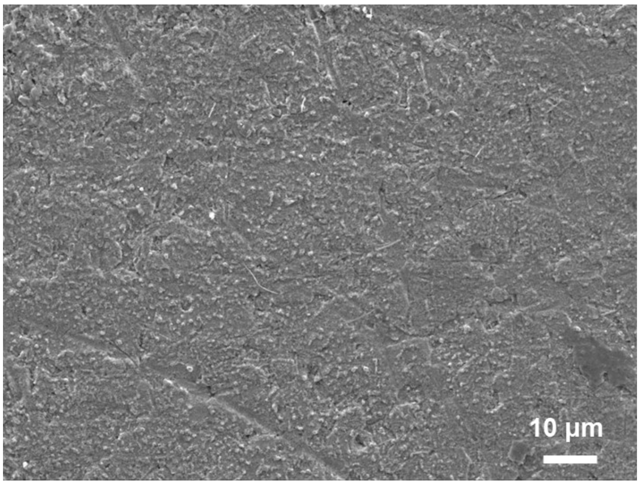

Fig. S17. Typical SEM image of Zn anode after 50 cycles with CPAN separator.

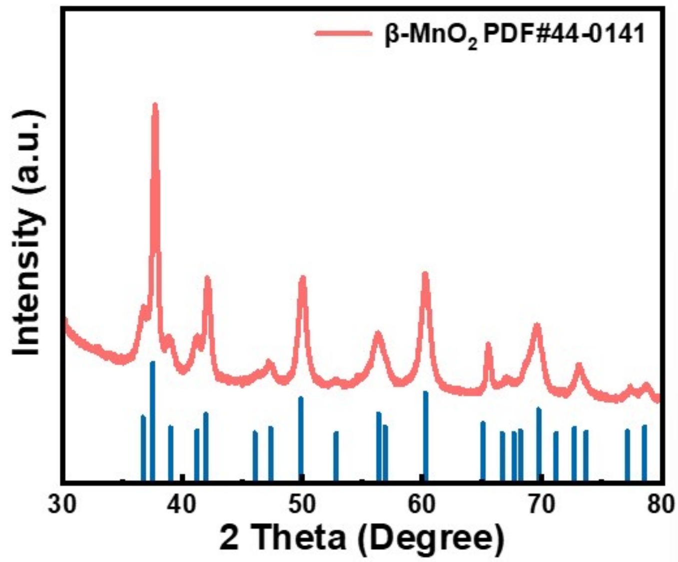

Fig. S18. XRD pattern of β-MnO_2 cathode.

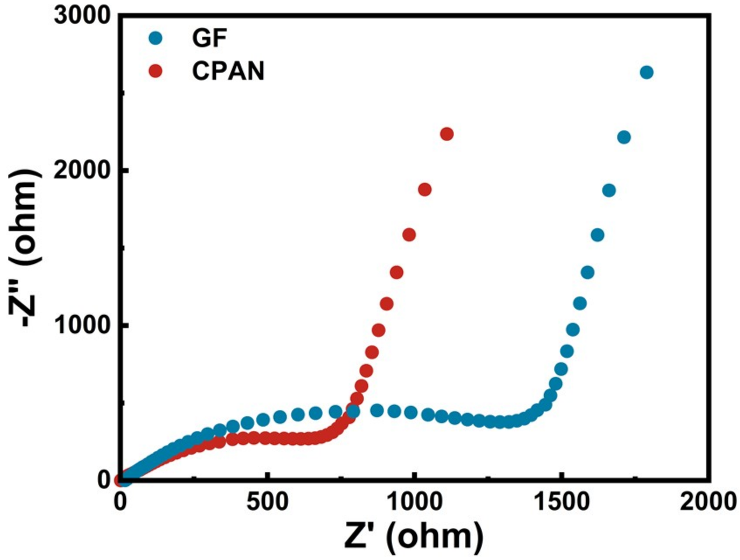

Fig. S19. The electrochemical impedance spectroscopy (EIS) spectra of full cells.

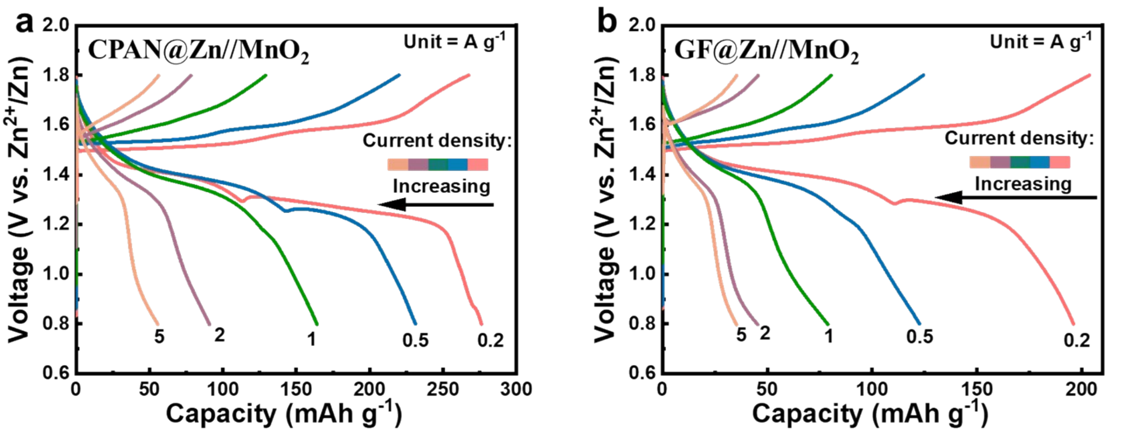

Fig. S20. Discharge/discharge curves of MnO_2||Zn full cells with (a) CPAN and (b) GF separator at different current density.

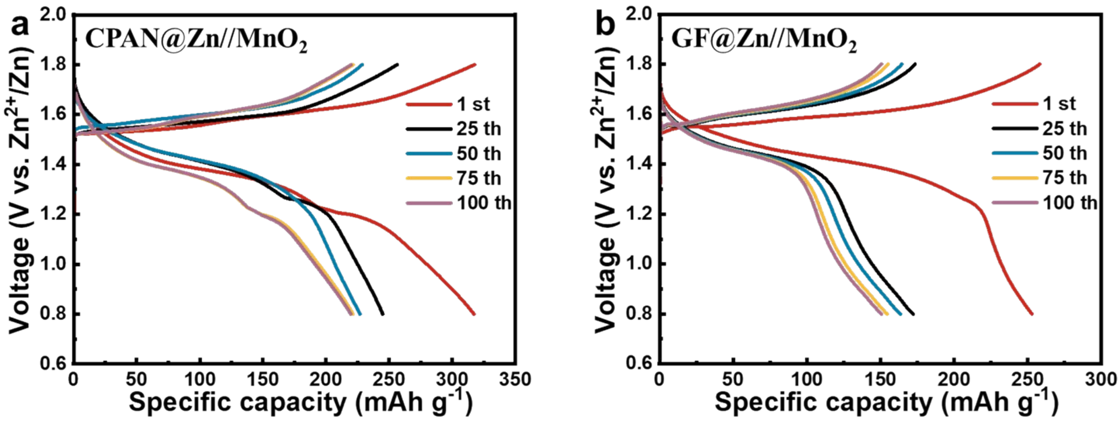

Fig. S21. Discharge/discharge curves of MnO_2||Zn full cell with (a) CPAN and (b) GF separator at 0.2 A g^{-1}.

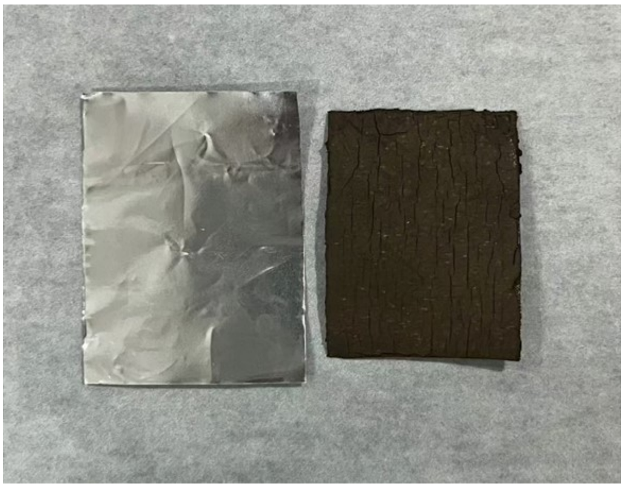

Fig. S22. Optical image of MnO_2 electrode.

Fig. S23. Photograph of MnO_2||Zn pouch cell under bending states.

Table S1. Performance of the zinc anodes with different separators.

Current (mA cm^{-2})	**Capacity (mAh cm^{-2})**	**Time (h)**	**Thickness (μm)**	**Maximum current**	**Ref.**
1	1	980	50	10	1
1	1	500	260	10	2
1	0.5	480	260	1	3
0.5	0.5	1150	50	5	4
0.2	0.05	1200	265	4	5
0.5	0.5	810	134	5	6
0.1	0.1	350	260	0.1	7
0.283		800	69	0.283	8
1	**1**	**1500**	**37**	**20**	**This work**

References

[1] J. F. Ma, X. Shi, Z. H. Wang, L. J. Zhou, X. G. Liu, X. H. Lu, Z. H. Jiang, Adv. Mater. 2024, **36**, 2406429.

[2] Z. C. Sun, J. Zhang, X. Y. Jiao, Z. J. Li, J. Energy. Storage 2024, **100**, 113780.

[3] L. Deng, K. L. Sun, J. Liu, Z. Y. Li, J. X. Cao, S. J. Liao, Molecules 2024, **29,** 3147.

[4] F. H. Wu, B. K. Wu, Y. B. Mu, L. F. Zou, J. F. He, M. Yang, L. Zeng, J. Power. Sources 2024, **597**, 234177.

[5] K. Yang, Z. Qu, Y. Li, B. Xue, X. P. Gu, Mater. Today. Chem. 2024, **42**, 102409.

[6] H. Zhang, J. B. Li, H. Z. Ren, J. X. Wang, Y. X. Gong, B. Wang, D. L. Wang, H. K. Liu, S. X. Dou, iScience 2024, **27**, 110237.

[7] N. Maeboonruan, J. Lohitkarn, C. Poochai, T. Lomas, A. Wisitsoraat, S. Kheawhom, S. Siwamogsatham, A. Tuantranont, C. Sriprachuabwong, J. Sci-Adv. Mater. Dev. 2022, **7**, 100467.

[8] Y. Fang, X. S. Xie, B. Y. Zhang, Y. Z. Chai, B. G. Lu, M. K. Liu, J. Zhou, S. Q. Liang, Adv. Funct. Mater. 2022, **32**, 2109671.